

Self induced temperature gradients in Brownian dynamics

Jack Devine

THE UNIVERSITY OF OTAGO



A THESIS SUBMITTED FOR HONOURS IN PHYSICS
AT THE UNIVERSITY OF OTAGO, DUNEDIN, NEW
ZEALAND

supervised by
Dr M. W. JACK

September 13, 2016

Abstract

Contents

1	Introduction	5
1.1	Brownian motion	5
1.2	Brownian motors	6
1.3	Classes of Brownian motors	7
1.3.1	Feynman ratchet and pawl fix this section up	7
1.3.2	Landauer's blowtorch expand	8
1.3.3	Tilted periodic potentials	9
2	System dynamics	11
2.1	The Smoluchowski equation	11
2.2	System thermodynamics	13
2.3	Dimensionalizing the equations	15
2.4	Steady state solution	16
2.5	Finite differences	18
2.6	Testing the numerics	20
2.6.1	A comparison with analytical results	20
2.6.2	Convergence tests	22
3	Exploration	25
3.1	Bistable potentials	25
3.1.1	Kramer's rate	25
3.2	The reverse Landauer blowtorch	27
3.3	Tilted periodic potentials	27
	Bibliography	29

Chapter 1

Introduction

1.1 Brownian motion

Brownian motion is the motion that occurs when looking at microscopic particles that are suspended in a fluid, this motion is highly random and is due to molecules in the fluid colliding with the particle trillions of times per second. In principle if one knew the momenta and positions of all particles in a system, then one could use Newtonian mechanics to fully predict the future state of the system. However, for systems of interest in this project, we will be looking at systems with particle number on the order of Avagadro's number ($N \sim 10^{23}$). With systems of this size, a Newtonian description is completely impractical, so instead we will use a statistical approach, in this view the motion of a single Brownian particle suspended in a fluid at a given temperature (which we will call the bath) is random.

Brownian motion was first observed by Robert Brown in 1827 [1], in these observations, Brown saw that microscopic particles (for example pollen grains) were in constant motion. He noticed that this motion was still present in inorganic material including granite and ground up Sphinx bones.

To mention all the mineral substances in which I have found these molecules, would be tedious; and I shall confine myself in this summary to an enumeration of a few of the most remarkable. These were both of aqueous and igneous origin, as travertine, stalactites, lava, obsidian, pumice, volcanic ashes, and meteorites from various localities. Of metals I may mention manganese, nickel, plumhago, bismuth, antimony, and arsenic. In a word, in every mineral which I could reduce to a powder, sufficiently fine to be temporarily suspended in water, I found these molecules more or less copiously; and in some cases, more particularly in siliceous crystals, the whole body submitted to examination appeared to be composed of them.

–**Robert Brown on what we now call Brownian particles**

Over half a century later, Einstein showed that Brownian motion was due to constant bombardment by water molecules in the surrounding environment

[2], Einsteins theory of Brownian motion was then experimentally verified by Perrin [3]. The trajectory of a single Brownian particle can either be described stochastically or an ensemble of Brownian particles can be described by a probability distribution. Work at around the same time by Smoluchowski allows us to determine the evolution of the probability distribution of a Brownian particle mathematically using the Smoluchowski equation which we will discuss in § 2.1. We will think of a Brownian particle moving in titled periodic potential of the form $V(x)$, as shown schematically in figure 1.1. In this figure we have a particle with a certain known probability density, the particle is agitated by thermal vibrations in a random diffusive manner, however there is also a forcing on the particles that we describe using the potential.

1.2 Brownian motors

Brownian motors are devices that can use stored chemical energy to create directed motion on a microscopic scale, they are ubiquitous in biology where they are used to perform important tasks in cells [4, 5] this is done by transforming energy from one degree of freedom to another. Recently, thanks to improvements in imaging techniques, researchers have been able to make highly detailed images of these motors and their working components [6]. As well as being able to crank a rotor in the in the fashion of a traditional motor, Brownian motors are also able to pump ions against a gradient and translocate molecules[5, 7–9]. Brownian motors have also been investigated in the laboratory, for example Ref [10] created a stochastic heat engine by placing a single colloidal particle in a time dependent optical trap. Likewise, Ref [11] placed a colloidal particle in an optical tweezer and drove the particle with explosive vaporization of the surrounding liquid, thus demonstrating a thermal mechanism for Brownian motors. Ref [12] placed DNA molecules in a time dependent potential to transport the molecules. Brownian ratchets capable of walking along a track have been implemented in the laboratory recently [13–15], in order to improve on these designs and to approach the efficiency present in nature, we will have to understand the physics of Brownian dynamics very clearly.

The name Brownian motors is not a misnomer, a Brownian motor can be modeled as a Brownian particle diffusing over its free energy landscape [7], in the case of Brownian motion it is natural to think of the particle moving in a spatial coordinate x , however in the case of Brownian motors the interpretation of the coordinate x is more abstract. In general x will be a degree of freedom for the system, examples include reaction coordinates for a chemical reactions, or in the case of a rotary motors, the angle of the motor itself.

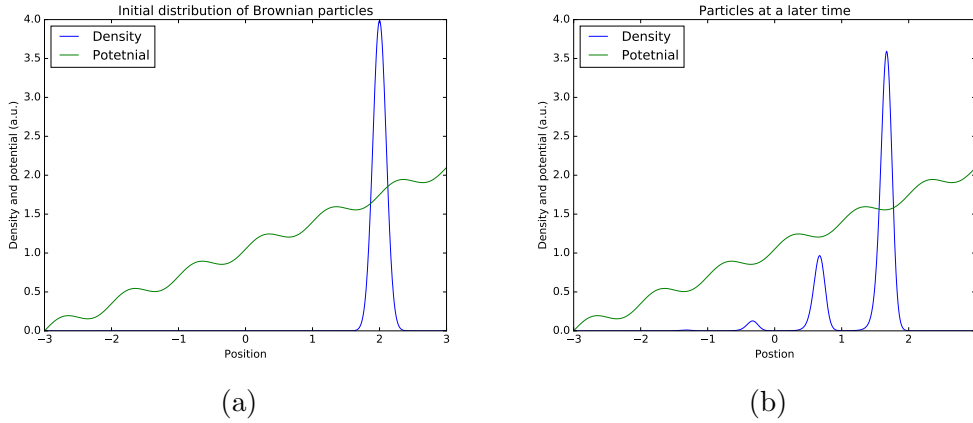


Figure 1.1: Schematic showing the probability density of particles diffusing in a one dimensional tilted periodic potential at a fixed temperature. We see that the particles tend to drift down the potential as they diffuse, this drift will be called the current J which we will quantify in section § 2.1.

1.3 Classes of Brownian motors

Here we will discuss different classes of Brownian motors and their relationship to this project. Different types of Brownian motors have been explored in the literature, including the Feynman ratchet [16], the Landauer blowtorch [17], thermal ratchets [11], time dependent potentials [10, 12] and tilted periodic potentials [5, 8].

1.3.1 Feynman ratchet and pawl fix this section up

The Feynman ratchet was initially discussed in the Feynman lectures [16] and was at first thought to be able to achieve greater than Carnot efficiency, however closer analysis showed that this was not possible [18]. The system works as follows, we have two boxes that are thermally insulated from one another that are connected by an axle that can rotate. In one box there is a ratchet and pawl connected to the axle that makes it easy for the axle to turn one way (say clockwise), but hard to turn the other way (anti-clockwise). In the other box the axle is connected to paddles that are being buffeted by a gas (which we call the bath). The motion of the paddles are random since they are dictated by Brownian motion, so the purpose of the ratchet and pawl is to rectify the Brownian motion of these paddles. One may think that this could be used to do work (for example by using the axle to lift a weight), however this is not true. The problem is that the ratchet and pawl themselves will also be subject to random motion so they will sometimes allow the axle to turn anti-clockwise. To model the Feynman ratchet, we will need two degrees of freedom [19], this is beyond the scope of this project because we will only simulate systems with one degree of freedom.

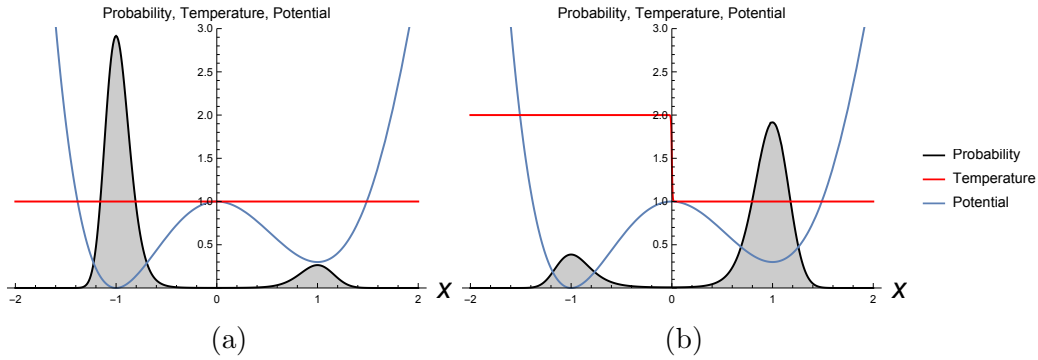


Figure 1.2: Landauer's blowtorch in a bi-stable potential: In (a) we see that if the particles are left for a long enough time, then they will reach an equilibrium where the population in the upper well is greater than that in the lower well. In (b) we see that if the temperature in the upper well is lower than that of the lower well, then the equilibrium concentrations can be drastically altered.

1.3.2 Landauer's blowtorch **expand**

The Landauer blowtorch scheme involves a temperature that varies in space [17]. The principle is shown schematically in Figure 1.2, in this figure the temperature is held fixed by an external heat source and can be made to vary along the potential. The steady state probability distribution was calculated using techniques that are described in § 2.4, in reference to this phenomena Landauer says that [17] “The relative occupation of competing states of local stability is not determined solely by the characteristics of the locally favored states, but depends on the noise along the whole path connecting the competing states.” The reason that particles move against the potential gradient is that where the potential is heated, the particles become more agitated, therefore we should expect that the probability of finding a particle in a hot region is small. A common analogy due to G. E. Hinton is pebbles on a driveway, if one places pebbles on a driveway in a uniform fashion, then after some time one will find that the pebbles will pile up on the side of the driveway where there is no traffic. This occurs despite the fact that the car exerts no net sideways force on the pebbles, the explanation of this phenomena is that the car is agitating the pebbles in the center effectively at random, but once the pebbles leave the center they experience no agitation (zero temperature) and so they will stay in place. This has caused some authors to describe the temperature as an effective potential [20, 21], in particular [22] report a so called reverse Landauer blowtorch effect. In this paper, the authors report show that if one begins with particles in the upper well of a bi-stable potential, then as the particles move to the lower well, they will reduce the temperature of the upper well. In section § 3.1, we will discuss the reverse Landauer blowtorch and it's effect on the Kramer's rate in more detail.

1.3.3 Tilted periodic potentials

The tilted periodic potential (Figure 1.1) is of particular interest for this project because it can be used to model biological motors [5, 8]. In this model, the potential can be a very complicated function of space despite the fact that temperature is held fixed. One way to model Brownian motors of this class is to think of a reaction coordinate x that describes the conformation of a molecule in a chemical reaction. An example of this is the reaction $\text{ATP} \rightleftharpoons \text{ADP} + \text{P}$, where ATP is adenosine tri-phosphate, ADP is adenosine di-phosphate and P is a lone phosphate molecule. This reaction coordinate is then coupled to a mechanical coordinate y so that each time that a reaction takes place, the motor will move in some way. Since this is a chemical reaction, the free energy will be decreased as time moves forwards. So a system that has a potential that is periodic in x is not sufficient to describe this situation, we will need to “tilt” the potential by adding a forcing f . The value of f will depend on the ΔG of the reaction (i.e. how far out of equilibrium the reaction is). It is shown in [5] that this can be modeled by the two dimensional Smoluchowski equation. In this project we will only be modeling the one dimensional Smoluchowski equation, so we will have to consider the case where x and y are tightly coupled. An example of tight coupling is the kinesin motor [8] that is used in cells to transport molecules. The kinesin motor is strongly bound to a track that it “walks” along, on each step the motor will hydrolyze an ATP molecule using the reaction shown above. This reaction liberates about $12k_B T$ Joules of energy that the motor uses to move forward. Kinesin motors are able to take many steps forward while taking few steps backwards all while falling off their track very infrequently [23].

Chapter 2

System dynamics

2.1 The Smoluchowski equation

As we will see, the diffusion is increased by increasing the temperature, while the derivative of the potential describes the external force on the particle. In some cases such as the Landauer blowtorch, the environment has a non uniform temperature held fixed by an external heat source [17]. With this in mind, we interpret Figure [make reference to Landauer blowtorch and explain how the project is different](#) 1.1 as follows: Brownian particles are subject to a given potential and are agitated by thermal noise, these agitations can give the particles the energy to move over barriers created by the potential. As one could imagine, these thermal interactions draw energy from the environment causing the temperature of the environment to change. Normally two simplifying assumptions are made at this point [7], (i) that the thermal fluctuations created by the motor are very small compared to the thermal energy of the surrounding environment which is assumed to be effectively infinite, (ii) that when these temperature fluctuations occur, they diffuse away so rapidly that they do not need to be accounted for. In this project, we will question the second assumption in the case of Brownian motors, the aims of this project are as follows:

- Determine a consistent physical description of Brownian motion involving self-induced temperature gradients, this description must be consistent with the laws of thermodynamics.
- Explore how this model differs from previous models of Brownian motion
- Determine conditions under which the model becomes the same as the previous models

This project will be focused on understanding the behavior of the coupled partial differential equations given by:

Put a reference to the Soluchowski equation earlier in the text, so that it is only reiterated here

$$J(x, t) = -\gamma^{-1} \frac{\partial}{\partial x} \left(\frac{\partial V(x, t)}{\partial x} P(x, t) + k_B T(x, t) \frac{\partial P(x, t)}{\partial x} \right) \quad (2.1)$$

$$\frac{\partial P(x, t)}{\partial t} = \frac{\partial J}{\partial x} \quad (2.2)$$

$$\frac{\partial T(x, t)}{\partial t} = -\kappa q(x, t) + D \frac{\partial^2 T(x, t)}{\partial x^2} \quad (2.3)$$

Where

- $P(x, t)$ is the probability density as a function of reaction coordinate x and time t
- $J(x, t)$ is called the current
- γ is the friction coefficient
- $V(x, t)$ is the potential for the motor
- k_B is the Boltzmann constant
- $q(x, t) = \partial_x V(x, t) J(x, t)$ is the heat from the motor
- κ is the thermal conductivity
- D is the thermal diffusivity

Equation (2.2) is called the Smoluschowski equation [24] and equation 2.3 is the heat equation. These equations make our intuitive notions more precise, we see that the first term on the right hand side of the Smoluchowski equation (equation 2.2) is a drift term that is forced by our potential and that the second term contains a diffusion term that is scaled by our temperature. In fact, Figure 1.1 was made by solving equation (2.2) numerically. Likewise, equation (2.3) also appeals to our intuition of how the motor should effect its environment. The first term represents the heat flux being produced by the motor [19], while the second term represents the diffusion of temperature into the environment. This model includes a temperature that depends on x and t , which has been explored in the literature [citations], where our model departs from previous work is that the temperature now depends on the evolution of the probability distribution as well. Coupled models of this type have been mentioned earlier by Streater [25, 26], our work uses a similar model.

2.2 System thermodynamics

Equation 2.2 and equation 2.3 define equations of motion for our system, the system may be confined to a region Ω embedded in a larger environment which interacts with our system through the boundary conditions. In this section, we will show that our equations of motion obey the first and second laws of thermodynamics. The potential energy of the particle is $U_P = \int_{\Omega} V(x)P(x)dx$ and the thermal energy of the bath is $c_p \int_{\Omega} T(x)dx$, where c_p is the specific heat capacity of the environment, with this we have.

$$E(t) = \int_{\Omega} V(x)P(x,t)dx + c_p \int_{\Omega} T(x,t)dx \quad (2.4)$$

By using the Smoluchowski equation and the heat equation, we can differentiate with respect to time to get:

$$\frac{dE}{dt} = \int_{\Omega} V(x) \frac{\partial P}{\partial t} dx + c_p \int_{\Omega} \frac{\partial T}{\partial t} dx \quad (2.5)$$

$$= - \int_{\Omega} V(x) \frac{\partial J}{\partial x} + c_p \int_{\Omega} -\kappa J(x) \frac{\partial V}{\partial x} + D \frac{\partial^2 T}{\partial x^2} dx \quad (2.6)$$

$$= [V(x)J(x)]_{\partial\Omega} + \int_{\Omega} \frac{\partial V}{\partial x} J(x) dx - \kappa c_p \int_{\Omega} \frac{\partial V}{\partial x} J(x) dx + D \left[\frac{\partial T}{\partial x} \right]_{\partial\Omega} \quad (2.7)$$

Notice that if the middle two terms cancel, then the change in energy is equal to the flow of energy through the boundaries. Thus, the first law of thermodynamics requires that $\kappa = \frac{1}{c_p}$, physically we can understand this by looking at the first term of equation 2.3. When the heat capacity is small, κ becomes large and in this case, even a small amount of heat being produced by the Brownian particle will have a large effect on the evolution of the temperature. Conversely, if the heat capacity is large, then the heat produced by the Brownian particle will have a very small effect on the temperature. We therefore expect that our model can be neglected in the case where the environment has a very large heat capacity compared to the heat being produced by the Brownian particle.

As for the entropy, we have [26]

$$S(t) = -k_B \int_{\Omega} P(x,t) \log(P(x,t)) dx + c_p \int_{\Omega} \log(T(x,t)) dx \quad (2.8)$$

The first term is the Gibbs energy in the continuous case [27] and the second term is the entropy of an incompressible fluid [28]. Differentiating with respect to time, we get

$$\frac{dS}{dt} = k_B \int_{\Omega} \frac{\partial J}{\partial x} + \frac{\partial J}{\partial x} \log P \, dx + c_p \int_{\Omega} \frac{1}{T} \left(-\kappa J \partial_x V + cD \frac{\partial^2 T}{\partial x^2} \right) dx \quad (2.9)$$

$$= k_B \left([J \log P]_{\partial\Omega} - \int_{\Omega} \frac{J}{P} \frac{\partial P}{\partial x} dx + [J]_{\partial\Omega} \right) - \int_{\Omega} \frac{J}{T} \frac{\partial V}{\partial x} + c_p D \int_{\Omega} \frac{1}{T} \frac{\partial^2 T}{\partial x^2} dx \quad (2.10)$$

We will denote the boundary terms with $B(t) = k_B([J \log P]_{\partial\Omega} + [\frac{\partial J}{\partial x}]_{\partial\Omega})$, now the change in entropy becomes:

$$\frac{dS}{dt} = - \int_{\Omega} \frac{J}{P} \frac{\partial P}{\partial x} + \frac{J}{T} \frac{\partial V}{\partial x} dx + cD \int_{\Omega} \frac{1}{T} \frac{\partial^2 T}{\partial x^2} dx + B(t) \quad (2.11)$$

$$= \int_{\Omega} \frac{J^2}{TP} dx + cD \int_{\Omega} \frac{1}{T} \frac{\partial^2 T}{\partial x^2} dx + B(t) \quad (2.12)$$

where in the second equality we used the fact that $J = P \frac{\partial V}{\partial x} + T \frac{\partial P}{\partial x}$. The first term on the right hand side is the entropy generated by the motor and the second is the entropy generated by temperature gradients, if no particles are flowing through the boundaries and if the nett heat flowing through the boundaries is zero, then the boundary terms vanish and we find that entropy always increases, in agreement with the second law of thermodynamics. Some authors write the Smoluchowski equation with $J = P \frac{\partial V}{\partial x} + T \frac{\partial P}{\partial x}$. By noticing that

$$\frac{\partial}{\partial x} \left(\frac{1}{T} \frac{\partial T}{\partial x} \right) = -\frac{1}{T^2} \left(\frac{\partial T}{\partial x} \right)^2 + \frac{1}{T} \frac{\partial^2 T}{\partial x^2} \quad (2.13)$$

we can rewrite the third term as:

$$c_p D \int_{\Omega} \frac{1}{T} \frac{\partial^2 T}{\partial x^2} dx = c_p D \int_{\Omega} \frac{\partial}{\partial x} \left(\frac{1}{T} \frac{\partial T}{\partial x} \right) + \frac{1}{T^2} \left(\frac{\partial T}{\partial x} \right)^2 dx \quad (2.14)$$

$$= c_p D \int_{\Omega} \frac{1}{T^2} \left(\frac{\partial T}{\partial x} \right)^2 dx + c_p D \left[\frac{1}{T} \frac{\partial T}{\partial x} \right]_{\partial\Omega} \quad (2.15)$$

which means that we can now absorb the third term into the boundary terms. If we define

$$\dot{S}_{gen} \equiv \int_{\Omega} \frac{J^2}{TP} + c_p D \frac{1}{T^2} \left(\frac{\partial T}{\partial x} \right)^2 dx \quad (2.16)$$

and

$$B(t) \equiv k_B \left([J \log P]_{\partial\Omega} + \left[\frac{\partial J}{\partial x} \right]_{\partial\Omega} \right) + c_p D \left[\frac{1}{T} \frac{\partial T}{\partial x} \right]_{\partial\Omega} \quad (2.17)$$

Then we notice that the change in entropy is equal to a positive number \dot{S}_{gen} plus the entropy flowing through the boundaries, this is precisely the second

law of thermodynamics. Furthermore, the generated entropy can be split into two terms, the first term is to be interpreted as the entropy generated by the Brownian particle, since the motion of the particle is random, as the Brownian particle diffuses we will become less certain of its position. The second term is the entropy generated by the diffusion of temperature gradients, if one studies the solutions to the heat equation, then one will find that any spikes in the temperature will flatten out and eventually the temperature will be flat. This flattening out of the temperature is naturally associated with an increase in entropy.

2.3 Dimensionalizing the equations

Upon viewing equations 2.2 and 2.3, we see that there is a large number of constants that are set by the properties of the Brownian particle that we are modeling. We would like to reduce the number of variables for two reasons (i) by reducing the number of variables we will hopefully gain a more concise physical description of the system (ii) having a small number of free variables is very convenient for creating a program to approximate the equations numerically, dimensionless equations tend to be less prone to numerical error because they avoid cases where small numbers are compared to large ones in a floating point system [citation] Here we will non-dimensionalize the equations, to do this, introduce $\bar{x} = \frac{x}{L}$, then the Smoluchowski equation becomes

$$\frac{\partial P}{\partial t} = \gamma^{-1} \frac{1}{L^2} \frac{\partial}{\partial \bar{x}} \left(P \frac{\partial V}{\partial \bar{x}} + k_B T \frac{\partial}{\partial \bar{x}} (P) \right) \quad (2.18)$$

Now let E_0 be the potential energy difference along one period, i.e. $E_0 = \max(v_0(x)) - \min(v_0(x))$. Now we will introduce the dimensionless potential and the dimensionless temperature as $\hat{V}(x) = \frac{V(x)}{E_0}$ and $\hat{T}(x) = \frac{k_B T(x)}{E_0}$ respectively. Now the Smoluchowski equation becomes

$$\frac{\partial P}{\partial t} = \frac{E_0}{\gamma L^2} \frac{\partial}{\partial \bar{x}} \left(P \frac{\partial \hat{V}}{\partial \bar{x}} + \hat{T} \frac{\partial P}{\partial \bar{x}} \right) \quad (2.19)$$

Let $\tau = \frac{E_0}{\gamma L^2}$ and $\hat{P} = LP$, with this we have:

$$\frac{\partial \hat{P}}{\partial \tau} = \frac{\partial}{\partial \bar{x}} \left(\hat{P} \frac{\partial \hat{V}}{\partial \bar{x}} + \hat{T} \frac{\partial \hat{P}}{\partial \bar{x}} \right) \quad (2.20)$$

Now we define $\hat{J} = \frac{\gamma L^2}{E_0} J$, applying these definitions to the equation for the temperature evolution, we find that:

$$\frac{E_0^2}{\gamma k_B L^2} \frac{\partial \hat{T}}{\partial \tau} = -\kappa \frac{E_0}{\gamma L^2} \hat{J}(\bar{x}) \frac{E_0}{L} \frac{\partial \hat{V}}{\partial \bar{x}} + \frac{D E_0}{k_B L^2} \frac{\partial^2 \hat{T}}{\partial \bar{x}^2} \quad (2.21)$$

Now let $\alpha = \frac{\kappa k_B}{L}$ and $\beta = \frac{D\gamma}{E_0}$, then we have

$$\frac{\partial \hat{T}}{\partial \tau} = -\alpha \hat{J}(\bar{x}) \frac{\partial \hat{V}}{\partial \bar{x}} + \beta \frac{\partial^2 \hat{T}}{\partial \bar{x}^2} \quad (2.22)$$

As for the energy of the system, the dimensioned version is:

$$E(t) = \int P(x)V(x)dx + \frac{1}{\kappa} \int T(x)dx \quad (2.23)$$

Let $\hat{E}(t) = \frac{E(t)}{E_0}$, we have:

$$\hat{E}(t) = \int \hat{P}\hat{V}d\bar{x} + \frac{L}{k_B\kappa} \int \hat{T}d\bar{x} \quad (2.24)$$

$$= \int \hat{P}\hat{V}d\bar{x} + \frac{1}{\alpha} \int \hat{T}d\bar{x} \quad (2.25)$$

So our system depends on the parameters α and β as well as the shape of the potential. Physically, α represents how much the particle interacts with the environment thermally and β represents how quickly the temperature diffuses.

2.4 Steady state solution

In order to see how the equations of motion behave with time, we have to resort to numerical methods (see section 2.5). However we note that for a given potential there will be a stationary solution that we will refer to as the “steady state”, given periodic boundary conditions, we will derive an analytical form for this steady state.

In the steady state, we have:

$$\frac{\partial P(x,t)}{\partial t} = 0 = \frac{\partial J}{\partial x} \quad (2.26)$$

$$\frac{\partial T(x,t)}{\partial t} = 0 = -\kappa q(x,t) + \frac{\partial}{\partial x} \left(D \frac{\partial T(x,t)}{\partial x} \right) \quad (2.27)$$

Suppose that we have the following boundary conditions:

$$P(x=0) = P(x=L) \quad (2.28)$$

$$J(x=0) = J(x=L) \quad (2.29)$$

$$\left. \frac{\partial T}{\partial x} \right|_{x=0} = 0 = \left. \frac{\partial T}{\partial x} \right|_{x=L} \quad (2.30)$$

where L is the length scale of the system. Physically, these conditions say that the nett current flowing out of the boundaries is zero and that no heat escapes

from the system, thus the energy of the sytem is conserved. Section 5.2 of [20] gives the steady state current as:

$$J_s = \left[\frac{2k_B T(L)}{\psi(L)} - \frac{2k_B T(0)}{\psi(0)} \right] P_s(0) \left[\int_0^L dx' / \psi(x') \right]^{-1} \quad (2.31)$$

with $\psi(x) \equiv \exp[-\int_0^x dx' \frac{\partial_x V(x')}{2k_B T(x')}]$. Meanwhile, the density is:

$$P_s(x) = P_s(0) \left[\frac{\int_0^x \frac{dx'}{\psi(x')} \frac{T(L)}{\psi(L)} + \int_x^L \frac{dx'}{\psi(x')} \frac{T(0)}{\psi(0)}}{\frac{T(x)}{\psi(x)} \int_0^L \frac{dx'}{\psi(x')}} \right] \quad (2.32)$$

In this case, J_s is a constant and $P_s(0)$ is also a constant. Assuming that we know these constants it is now possible to find the steady state temperature. We have:

$$\frac{\partial T}{\partial t} = 0 = -\kappa J_s \partial_x V + D \frac{\partial^2 T}{\partial x^2} \quad (2.33)$$

In one dimension, 2.33 can be written as an ordinary differential equation of the form

$$T''(x) = \frac{\kappa J_s}{D} V'(x) \quad (2.34)$$

We can solve this equation by integrating both sides twice to give:

$$T(x) = \frac{\kappa J_s}{D} \int_0^x V(x') dx' + \xi x + d \quad (2.35)$$

for unkown constants ξ and d . By applying the boundary condition 2.30, we find that

$$T'(0) = 0 = \frac{\kappa J_s}{D} V(0) + \xi \quad (2.36)$$

$$T'(L) = 0 = \frac{\kappa J_s}{D} V(L) + \xi \quad (2.37)$$

This implies that either $J_s = 0$ or $V(0) = V(L)$, meaning that the coupled system does not admit a steady state solution for a tilted potential. Later, we will see that it is possible to have a steady state in higher dimensions where the flow of heat from the environment can dissipate the heat produced by the Brownian particle. By recalling that $E = \int_0^L P(x') V(x') dx' + c \int_0^L T(x') dx'$ we are able to find an expression for d . First, we will integrate the temperature from 0 to L

$$\int_0^L T(x') dx' = \frac{\kappa J_s}{D} \int_0^L dx' \int_0^{x'} V(x'') dx'' + \xi \frac{L^2}{2} + dL \quad (2.38)$$

Therefore,

$$d = \frac{1}{L} \left(cE - c \int_0^L P(x') V(x') dx' - \frac{\kappa J_s}{D} \int_0^L dx' \int_0^{x'} V(x'') dx'' + \xi \frac{L^2}{2} \right) \quad (2.39)$$

It would seem that one should be able to calculate the steady state current and density directly from the equations shown above. However, we notice that the constants J_s and $P_s(0)$ have to satisfy equations (2.31), (2.32) and (2.35) while also satisfying the normalization condition $\int_0^L P(x)dx = 1$. To do this we define an objective function given by

$$obj(J_s, P_s(0)) = \left(J_s - \left[\frac{2k_B T(L)}{\psi(L)} - \frac{2k_B T(0)}{\psi(0)} \right] P_s(0) \left[\int_0^L dx' / \psi(x') \right]^{-1} \right)^2 \quad (2.40)$$

And we minimize this objective function with respect to J_s and $P_s(0)$ under the constraint $\int_0^L P(x)dx = 1$. Another way to do this is to guess a steady state density and temperature and use finite differencing to simulate forward in time until the transients die out.

2.5 Finite differences

The one dimensional equation can be solved on a discrete grid by using the finite differences method, the main idea behind this strategy is to approximate derivatives with equations of the form:

$$\frac{df}{dx} \approx \frac{f(x-h) - f(x+h)}{2h} \quad (2.41)$$

for some small h , likewise the second derivative of a function is approximated with

$$\frac{d^2 f}{dx^2} = \frac{f(x-h) - 2f(x) + f(x+h)}{h^2} \quad (2.42)$$

In our simulations, we will use the Crank Nicolson scheme to solve the equations. From now on, we will use the notation that $F(j\Delta x, n\Delta t) = F_j^n$, the key equation for the Crank Nicolson scheme is:

$$\frac{P_j^{n+1} - P_j^n}{\Delta t} = \frac{1}{2}(F_j^{n+1} + F_j^n) \quad (2.43)$$

where F represents the right hand side of the equation that we are doing finite differences on. By applying finite differences to the dimensionless Smoluchowski equation (eq 2.20), we find that:

$$F_j^i = \frac{P_{j+1}^i \partial V_{j+1}^i - P_{j-1}^i \partial V_{j-1}^i}{2\Delta x} + \frac{T_{j+1}^i - T_{j-1}^i}{2\Delta x} \frac{P_{j+1}^i - P_{j-1}^i}{2\Delta x} + T_j^i \frac{P_{j+1}^i - 2P_j^i + P_{j-1}^i}{\Delta x^2} \quad (2.44)$$

where we omitted the hats for notational convenience. We make the following definitions:

$$\begin{aligned}
a_j^{n+1} &= \frac{-2T_j^{n+1}}{\Delta x^2} \\
b_j^{n+1} &= \frac{\partial_x V_{j+1}^{n+1}}{2\Delta x} + \frac{T_{j+1}^{n+1} - T_{j-1}^{n+1}}{4\Delta x^2} \\
c_j^{n+1} &= -\frac{\partial_x V_{j-1}^{n+1}}{2\Delta x} - \frac{T_{j+1}^{n+1} - T_{j-1}^{n+1}}{4\Delta x^2} \\
a_j^n &= \frac{-2T_j^n}{\Delta x^2} \\
b_j^n &= \frac{\partial_x V_{j+1}^n}{2\Delta x} + \frac{T_{j+1}^n - T_{j-1}^n}{4\Delta x^2} \\
c_j^n &= -\frac{\partial_x V_{j-1}^n}{2\Delta x} - \frac{T_{j+1}^n - T_{j-1}^n}{4\Delta x^2}
\end{aligned} \tag{2.45}$$

With these definitions, the Crank Nicolson scheme can be written down as follows:

$$-\frac{\Delta t}{2}a_j^{n+1}P_{j-1}^{n+1} + \left(1 - \frac{\Delta t}{2}b_j^{n+1}\right)P_j^{n+1} - \frac{\Delta t}{2}c_j^{n+1}P_{j+1}^{n+1} = a_j^n P_{j-1}^n + \left(1 + \frac{\Delta t}{2}b_j^n\right)P_j^n + \frac{\Delta t}{2}c_j^n P_{j+1}^n \tag{2.46}$$

This equation can be written in matrix form by defining the following matrices:

$$A = \begin{bmatrix} a_0^{n+1} & b_1^{n+1} & 0 & 0 & 0 & \dots & 0 \\ c_0^{n+1} & a_1^{n+1} & b_2^{n+1} & 0 & 0 & \dots & 0 \\ 0 & c_1^{n+1} & a_2^{n+1} & b_3^{n+1} & 0 & \dots & 0 \\ \vdots & \vdots & \ddots & \ddots & \ddots & \vdots & \vdots \\ 0 & \dots & \dots & c_{J-2}^{n+1} & a_{J-1}^{n+1} & b_J^{n+1} \\ 0 & \dots & \dots & \dots & c_{J-1}^{n+1} & a_J^{n+1} \end{bmatrix}, \quad P^{n+1} = \begin{bmatrix} P_0^{n+1} \\ P_1^{n+1} \\ \vdots \\ P_{J-1}^{n+1} \\ P_J^{n+1} \end{bmatrix} \tag{2.47}$$

$$B = \begin{bmatrix} a_0^n & b_1^n & 0 & 0 & 0 & \dots & 0 \\ c_0^n & a_1^n & b_2^n & 0 & 0 & \dots & 0 \\ 0 & c_1^n & a_2^n & b_3^n & 0 & \dots & 0 \\ \vdots & \vdots & \ddots & \ddots & \ddots & \vdots & \vdots \\ 0 & \dots & \dots & c_{J-2}^n & a_{J-1}^n & b_J^n \\ 0 & \dots & \dots & \dots & c_{J-1}^n & a_J^n \end{bmatrix}, \quad P^n = \begin{bmatrix} P_0^n \\ P_1^n \\ \vdots \\ P_{J-1}^n \\ P_J^n \end{bmatrix} \tag{2.48}$$

With these matrices the equation now becomes,

$$\left(\mathbb{1} - \frac{\Delta t}{2} A \right) \cdot P^{n+1} = \left(\mathbb{1} + \frac{\Delta t}{2} B \right) \cdot P^n \quad (2.49)$$

we interpret this equation as saying that half of a backwards Euler step acting on P^{n+1} is equal to half of a forward Euler step acting on P^n . We write the equation to step P forward one time step as

$$P^{n+1} = \frac{\mathbb{1} + \frac{\Delta t}{2} B}{\mathbb{1} - \frac{\Delta t}{2} A} P^n \quad (2.50)$$

Each time that we step forward using this equation we will be out by a factor, this means that at each step we will need to renormalize using the equation $\int P(x) dx = 1$.

Likewise, we can apply the Crank Nicolson scheme to the heat equation, (eq 2.22), by looking at the right hand side of this equation, we find that

$$F_j^i = -\alpha \left(P_j^i (\partial_x V_j^i)^2 + \frac{T_{j+1}^i - T_{j-1}^i}{2\Delta x} \partial_x V_j^i \right) + \beta \frac{T_{j+1}^i - T_j^i + T_{j-1}^i}{\Delta x^2} \quad (2.51)$$

Just like the discretized Smoluchowski equation, these equations can be written in matrix form. The temperature is normalized by assuming that the energy remains fixed, this will be true as long as no heat or current flows through the boundaries, i.e. $J(x=a) = 0 = J(x=b)$ and $\frac{\partial T}{\partial x}|_a = 0 = \frac{\partial T}{\partial x}|_b$. In this case, the energy is constant and is given by $E = \int P(x) V(x) dx + c_p \int T(x) dx$, so each time that we step the temperature forward, we have to calculate the potential and thermal energy and then scale the temperature so that the total energy remains fixed.

Fortunately the matrices that we are dealing with are very sparse, so the program used to solve these equations can save on memory by calling sparse matrix libraries.

2.6 Testing the numerics

The idea behind finite differences is that as the discretization size goes to zero, the numerical approximation should converge on the correct analytical solution. We will compare our numerics with some known analytical results as well as performing convergence tests.

2.6.1 A comparison with analytical results

The Smoluchowski equation has a steady state probability density that takes on the form

$$P_{ss}(x) = N \exp \left(- \int_a^x \frac{V'(x')}{T(x')} dx' \right) \quad (2.52)$$

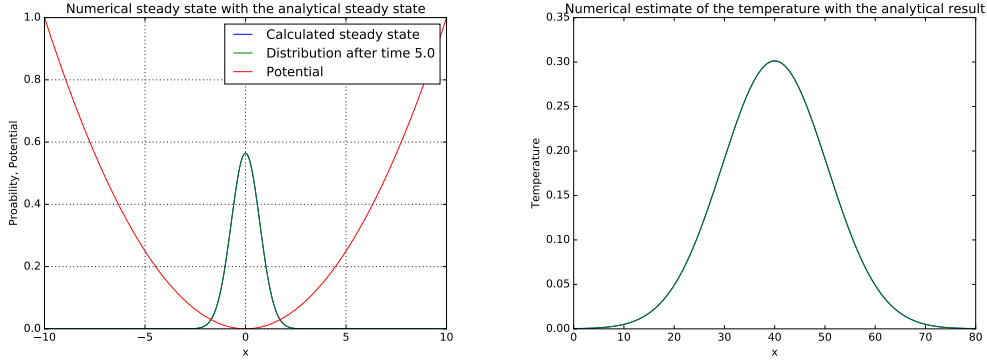


Figure 2.1: Finite differences in the steady state: The steady state for the system was calculated using equation 2.52, we start the system off in this state and then simulate the system forward 50,000 steps with $\Delta t = 10^{-4}$ and $\Delta x = 0.02$. (a) shows the analytical steady state with the state after the simulation, (b) shows the absolute difference between these two vectors. Even after 50,000 steps the system has not deviated from the analytical steady state significantly.

Figure 2.1 shows the a simulation where we began the system in the analytically calculated steady state, we then used finite differences to step forward 50,000 steps with $\Delta t = 10^{-4}$. After this simulation, we only found a minimal divergence from the steady state.

The heat equation can be solved using a Fourier series technique

$$\frac{\partial T}{\partial t} = \beta \frac{\partial^2 T}{\partial x^2} \quad (2.53)$$

the initial condition for the temperature will be denoted by,

$$T(x, 0) = f(x) \quad (2.54)$$

Lets say that the boundaries are at $x = \pm\infty$ and that the derivative of the temperature is zeros at the boudaries. The solution to the heat equation is given by:

$$T(x, t) = \sum_{n=1}^{\infty} D_n \sin\left(\frac{n\pi x}{L}\right) \exp\left(\frac{-n^2\pi^2\beta t}{L^2}\right) \quad (2.55)$$

where

$$D_n = \frac{2}{L} \int_0^L f(x) \sin\left(\frac{n\pi x}{L}\right) dx \quad (2.56)$$

We can compare these analytical results to the numerical ones obtained through finite differences, this is done in Figure 2.1

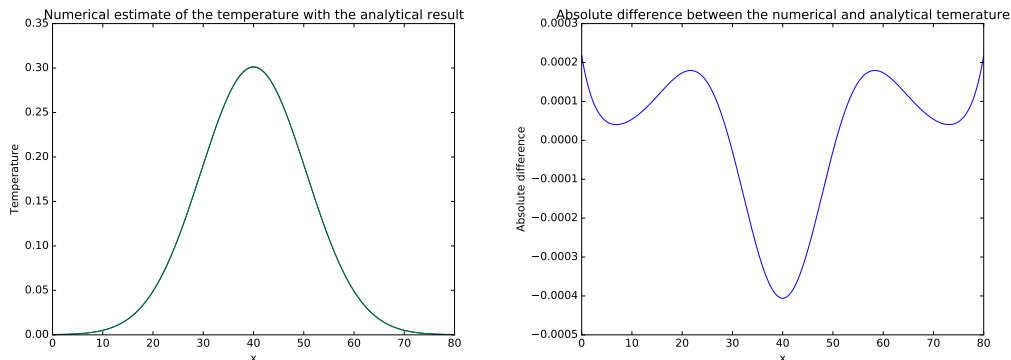


Figure 2.2: Finite differences on the heat equation: We simulate a situation where there are no sources for the heat equation and use equation 2.55 to obtain the analytical result we then compare this to the result of finite differences with $\Delta t = 10^{-2}$ and $\Delta x = 0.02$.

2.6.2 Convergence tests

The idea of finite differences is that as the step size goes to zero, the numerical approximation will converge on the correct solution to the underlying equation being approximated. In the previous section we showed that finite differences approximated the solution very closely in some instances where the analytical result could be obtained. In general, we will not have an analytical solution to compare to but we would still like to be able to quantify the performance of our techniques.

Convergence tests involve decreasing the discretization size and checking whether the numerical solutions converge at all. In Figure 2.3, the Smoluchowski equation was simulated while keeping the temperature fixed, each time we halve Δt and measure the normed difference between the new result and the previous one.

Likewise, we can do convergence tests for the coupled system, for brevity we have only included the results for the evolution of the temperature. All of these plots show that the approximation converges exponentially to the solution.

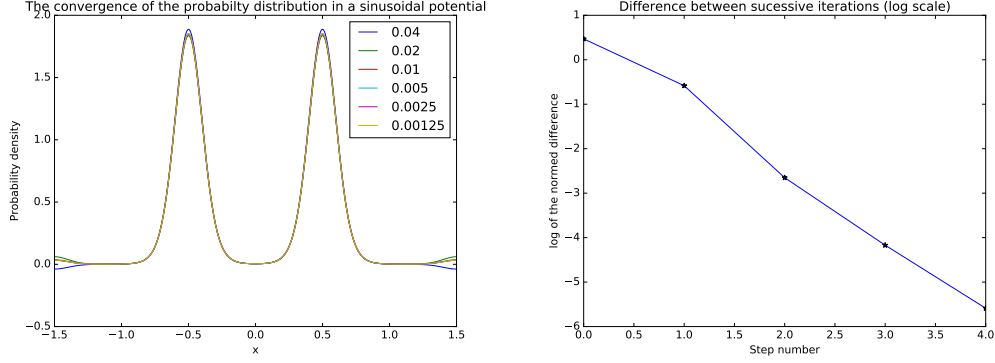


Figure 2.3: The convergence of the probability distribution as Δt is decreased, the spatial discretization Δx is kept constant at 0.006. (a) the Smoluchoski equation is simulated forward for 1.0 seconds each line shows the result with a different value of the time step Δt . (b) the normed difference between each of the successive vectors is calculated and the result is plotted on a log scale, the slope of this graph is called the convergence rate.

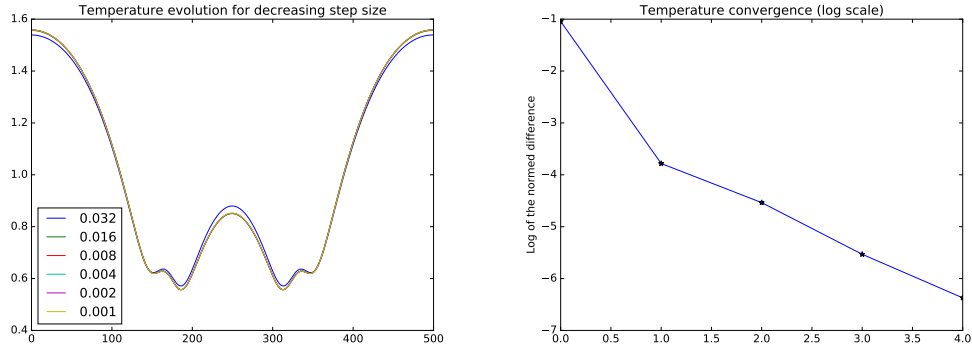


Figure 2.4: The convergence of the temperature as Δt is decreased, the spatial discretization Δx is kept constant at 0.006. (a) the coupled equations are simulated forward for 1.0 seconds each line shows the temperature with a different value of the time step Δt . (b) the normed difference between each of the successive vectors is calculated and the result is plotted on a log scale.

Chapter 3

Exploration

3.1 Bistable potentials

A bistable potential one that has two stable minima and an intermediate unstable maximum, these potentials occur in a wide range of applications including digital logic [29], protein folding [30] and chemical reactions [31]. The bistable potential well is one of the simplest ways to approach the Kramer's rate and many other important properties of a system [citations]. In the context of Brownian motion, understanding the nature of bistable potentials can help one to build a master equation describing more complicated potentials comprised of multiple deep wells [32, 33].

3.1.1 Kramer's rate

Consider the potential shown in Figure 3.1, if we begin in a state where we are certain that the particle is in the upper well, then as time passes, we should expect the probability distribution to move from point a over the barrier at b and into the well at point c . We will consider the regime where $E_B^+ = V(x_b) - V(x_a) \gg k_B T$, in this regime the rate at which the particles flow from a to c is given by the Eyring-Kramers law [34, 35], for our dimensionless equations, this has the form,

$$\kappa_+ = \frac{\sqrt{-V''(x_b)V''(x_a)}}{2\pi} \exp\left(\frac{-E_B^+}{T}\right) \quad (3.1)$$

Likewise, there will be a current flowing from c to a , we will denote this by κ_- , once we have calculated both of these rates, the population in the upper well will be given by:

$$P_+(t) = \exp((\kappa_+ - \kappa_-)t). \quad (3.2)$$

We can also achieve this result numerically by starting the system off in the upper well and simulating forward while calculating the probability that the

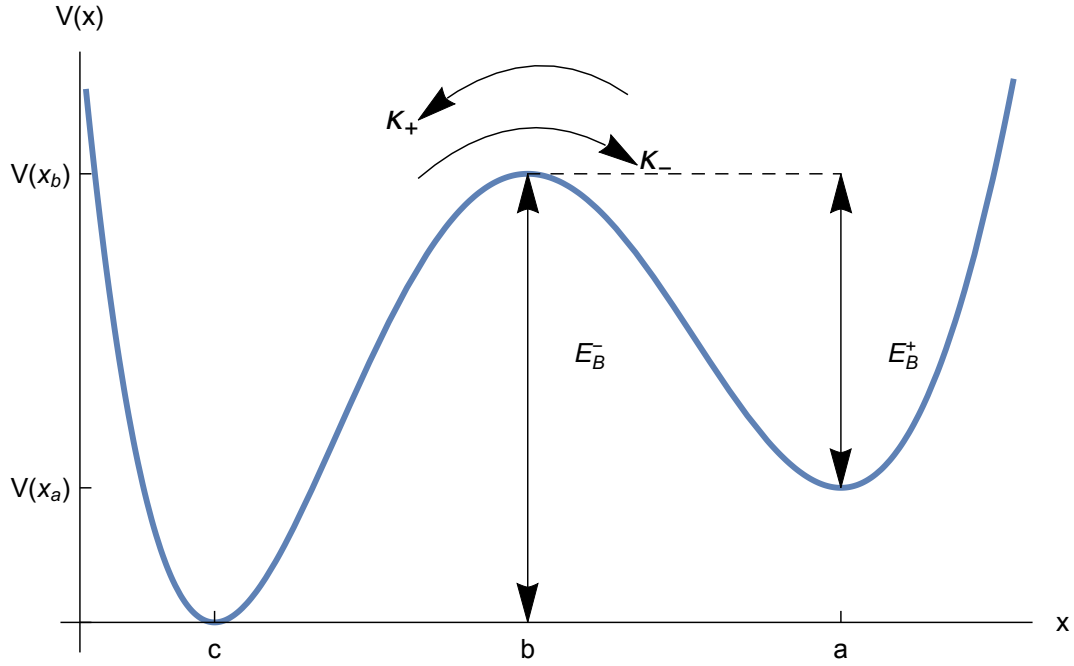


Figure 3.1: Bistable potential: In this plot we show the potential where we explore the Kramers rate, the potential has local minima at a and c and a maximum at b . If we begin with a probability distribution in the upper well, then the distribution will decay into the ground state of the upper well and then begin to decay into the lower well. The rate of flow from the upper well to the lower one will be denoted by κ_+ and the rate of flow from the lower well into the upper one will be denoted by κ_- .

particle is in the upper well at each step. We then fit an exponential to this data and the fitted rate will be our numerically estimated Kramers rate. To assist with measuring the Kramer's rate, we used Hermite interpolation to create a sixth order polynomial with the desired bistable shape. Specifically, we would allow $V(x)$ to be a general 6th order polynomial and then we would specify the value of the polynomial at the locations a , b and c , we would also enforce that the first derivative vanished at these locations. This would yield 6 equations which we would solve to give us the coefficients of $V(x)$, an example of such a polynomial is shown in Figure 3.1. Using these interpolating polynomials, we could keep the locations of the wells fixed while controlling the barrier height E_B^+ . Once we had a potential, we would place the probability distribution in the upper well and then measure the probability that the particle is in the upper well with time and use this information to obtain the Kramer's rate, as shown in Figure [make this figure](#). This same technique can be used to obtain the Kramer's rate when the temperature is not held fixed. In this case, the Kramer's rate is sensitive to the boundary conditions imposed on the temperature and on the precise values of α and β as shown in Figure [make this figure](#).

3.2 The reverse Landauer blowtorch

As noted in subsection 1.3.2, the relative occupancy of wells depends on the spatial distribution of the temperature meaning that the temperature can act as a pseudo-force. However, it has been noted that when the movement of the particle has an effect on the environment, the opposite effect can occur [22]. Concretely, the authors claim that if the probability distribution begins in the upper well, then after they have moved into the lower well they will cause the upper well to become colder in a process called Brownian cooling. In this paper, the authors treat the system stochastically and are not able to model the diffusion of temperature. This is the same as our model with β in equation ?? set to zero. Here we will show that this approximation does not always yield an accurate description of the physics involved.

3.3 Tilted periodic potentials

Tilted periodic potentials are very important in biology where they can be used to model molecular motors.

Bibliography

- [1] Robert Brown. A brief account of microscopical investigations on the particles contained in the pollen of plants. *Privately circulated in 1828*, 1828.
- [2] A Einstein. On the movement of small particles suspended in stationary liquids required by the molecular-kinetic theory of heat. *Ann. Phys.*, 17:549–560, 1905.
- [3] Jean Perrin. *Brownian movement and molecular reality*. Courier Corporation, 2013.
- [4] Rob Phillips and Stephen R. Quake. The Biological Frontier of Physics. *Physics Today*, May 2006.
- [5] Marcelo O. Magnasco. Molecular combustion motors. *Physical Review Letters*, 1994.
- [6] Anke Treuner-Lange Janet Iwasa Lotte Søggaard-Andersen Grant J. Jensen Yi-Wei Chang, Lee A. Rettberg. Architecture of the type IVa pilus machine. *Science*, 2016.
- [7] Peter Reimann. Brownian Motors: noisy transport far from equilibrium. *Physics Reports*, 2001.
- [8] S Leibler and D A Huse. Porters versus rowers: a unified stochastic model of motor proteins. *The Journal of Cell Biology*, 121(6):1357–1368, 1993.
- [9] S Leibler and DA Huse. A physical model for motor proteins. *Comptes rendus de l'Academie des sciences. Serie III, Sciences de la vie*, 313(1):27–35, 1990.
- [10] Valentin Blickle and Clemens Bechinger. Realization of a micrometre-sized stochastic heat engine. *Nature Physics*, 2011.
- [11] Pedro A. Quinto-Su. A microscopic steam engine implemented in an optical tweezer. *Nature Communications*, 2014.

- [12] Steven A. Henck Michael W. Deem Gregory A. McDermott James M. Bustillo John W. Simpson Gregory T. Mulhern Joel S. Bader, Richard W. Hammond and Jonathan M. Rothberg. Dna transport by a micromachined Brownian ratchet device. *PNAS*, 1999.
- [13] Zhisong Wang. Bio-inspired track-walking molecular motors (perspective). *Biointerphases*, 5(3):FA63–FA68, 2010.
- [14] Max von Delius, Edzard M Geertsema, and David A Leigh. A synthetic small molecule that can walk down a track. *Nature chemistry*, 2(2):96–101, 2010.
- [15] Max von Delius, Edzard M Geertsema, David A Leigh, and Dan-Tam D Tang. Design, synthesis, and operation of small molecules that walk along tracks. *Journal of the American Chemical Society*, 132(45):16134–16145, 2010.
- [16] Richard Feynman. *Feynman lectures on physics*. California Institute of Technology, 1963.
- [17] Rolf Landauer. Motion out of noisy states. *Journal of Statistical Physics*, 53(1):233–248, 1988.
- [18] Juan M. R. Parrondo and Pep Español. Criticism of Feynman’s analysis of the ratchet as an engine. *American Journal of Physics*, 64(9):1125–1130, 1996.
- [19] C. Tumlin M. W. Jack. Intrinsic irreversibility limits the efficiency of multi-dimensional brownian motors. *Physical Review E*, 2016.
- [20] Crispin Gardiner. *Stochastic methods*. Springer, 2009.
- [21] NG van Kampen. Explicit calculation of a model for diffusion in non-constant temperature. *Journal of mathematical physics*, 29(5):1220–1224, 1988.
- [22] Moupriya Das, Debojyoti Das, Debashis Barik, and Deb Shankar Ray. Landauer’s blowtorch effect as a thermodynamic cross process: Brownian cooling. *Phys. Rev. E*, 92:052102, Nov 2015.
- [23] Schnapp BJ. Block SM, Goldstein LS. Bead movement by single kinesin molecules studied with optical tweezers. *Nature*, 1990.
- [24] David Keller and Carlos Bustamante. The Mechanochemistry of Molecular Motors. *Biophysical Journal*, 2000.
- [25] R. F. Streater. Non linear heat equations. *Reports on Mathematical Physics*, 1997.

- [26] R. F. Streater. A Gas of Brownian Particles in Statistical Dynamics. *Journal of Statistical Physics*, 1997.
- [27] Edward T Jaynes. Gibbs vs boltzmann entropies. *American Journal of Physics*, 33(5):391–398, 1965.
- [28] Yunus A Cengel and Michael A Boles. Thermodynamics: an engineering approach. *Sea*, 1000:8862, 1994.
- [29] Christopher J Myers, Michele Celebrano, and Madhavi Krishnan. Information storage and retrieval in a single levitating colloidal particle. *Nature nanotechnology*, 10(10):886–891, 2015.
- [30] Joseph D Bryngelson and Peter G Wolynes. Intermediates and barrier crossing in a random energy model (with applications to protein folding). *The Journal of Physical Chemistry*, 93(19):6902–6915, 1989.
- [31] Bruce J Berne and Robert Pecora. *Dynamic light scattering: with applications to chemistry, biology, and physics*. Courier Corporation, 1976.
- [32] Victor Barcilon. Eigenvalues of the one-dimensional smoluchowski equation. *Journal of Statistical Physics*, 82(1):267–296, 1996.
- [33] Katharine J Challis and Michael W Jack. Energy transfer in a molecular motor in kramers’ regime. *Biophysical Journal*, 106(2):371a–372a, 2014.
- [34] Henry Eyring. The activated complex in chemical reactions. *The Journal of Chemical Physics*, 3(2):107–115, 1935.
- [35] Hendrik Anthony Kramers. Brownian motion in a field of force and the diffusion model of chemical reactions. *Physica*, 7(4):284–304, 1940.